

Influence of matrix absorbance on the near-field and spectral characteristics of plasmon spherical nanoparticles scattering

© R.A. Dynich¹, A.N. Ponyavina²

¹ Belarusian State University of Informatics and Radioelectronics, Minsk, Belarus

² Stepanov Institute of Physics, Belarusian Academy of Sciences, Minsk, Belarus

e-mail: radynich@gmail.com

Received June 24, 2022

Revised August 17, 2022

Accepted September 2, 2022

Regularities of a size dependence of extinction and absorption efficiency factors as well as of near-zone and far-zone scattering efficiency factors are studied in the spectral range of the surface plasmon resonance of absorption (SPRA) for silver spherical nanoparticles placed into absorbing matrixes with complex refraction index $n_m + i\kappa_m$. Numerical simulation was made with the use of the Mie theory for absorbing matrixes. Approximation of the electron mean free path limitation was used in order to take into account the intrinsic size effects into a metal nanoparticle which consist in a size dependence of its dielectric characteristics. We shown that a growth of matrix absorbency leads to a strong suppression of resonances of extinction Q_{ext} and near-zone scattering Q_{NF} efficiency factors without any essential changing of their spectral position. We established that for any fixed wavelength in the spectral range of the SPRA the values of Q_{ext} and Q_{NF} depend on metal nanoparticle sizes nonmonotonically at $\kappa_m = 0-0.1$. The R_{NP} optimal value, which corresponds to the maximal values of efficiency factors for the given material of plasmonic nanoparticles, increases at the matrix absorbency growth. The intrinsic size effects contribution to the efficiency factors resonance suppression decreases at the enhancement of nanoparticle sizes and/or matrix absorption. As an example of a real absorbing matrix with a dispersion of refraction index we considered the nickel phtalocyanine matrix (NiPc), which is interesting from the point of view of photovoltaic applications.

Keywords: Plasmonic nanoparticles, absorbing matrixes, characteristics of near-zone and far-zone scattering.

DOI: 10.21883/EOS.2022.11.55100.3864-22

Introduction

At present, it is well known that noble metal nanoparticles are characterized by the presence of plasmon surface resonance of absorption and scattering in the optical region of the spectrum. In this spectral region, local electromagnetic fields near the surface of nanoparticles are significantly enhanced [1–3]. The physical cause of resonant attenuation of light by noble metal nanoparticles is coherent oscillations of conduction electrons stimulated by incident optical radiation and extremely sensitive to the shape, size of nanoparticles and properties of the environment [4].

The sensitivity of the surface plasmonic resonance (SPR) bands of plasmonic metal nanoparticles to the dielectric properties of the environment is being actively studied and is already being used in nanophotonics and optoelectronics, for example, for sensorics in chemistry, biology and medicine [5]. Plasmonic nanostructures are successfully used as substrates for giant Raman scattering (GRS) and light-emitting devices [6]. The possibility of amplifying the local field near metal nanoparticles also turned out to be attractive for use in photovoltaic solar cells, since the amplified field increases the absorption in the semiconductor matrix. This is one of the intensively developed concepts for increasing the efficiency gains of solar energy conversion

both based on traditional semiconductors and in thin-film cells based on organic semiconductors [7–9].

Experimentally, the change in the absorption and conductivity of thin films of organic semiconductors when they are doped with plasmonic nanoparticles was studied in [10–13]. It was found that the presence of plasmonic nanoparticles in the composite significantly affects the spectral characteristic, resulting in the long-wavelength relative to the SPR spectral region to a significant absorbance increase compared to the simple additive summation of the intensities of the SPR band of Ag nanoparticles and the absorption bands of the organic component. Such an increase in the absorbance of the hybrid composite is associated with the near-field effect, which consists in an increase in absorption by the organic film due to an increase in the local field near the surface of plasmonic nanoparticles, which stimulates the processes of energy and charge carrier transfer in such structures.

At the same time, the theoretical aspects of the effect of absorption in a matrix on the characteristics of the SPR bands and the near-field characteristics are only just beginning to be studied. It has been defended in the works [14–18] that in the case of absorbing matrixes, the availability of additional dependence of the field on spatial coordinates complicates the procedure for calculating the characteristics of scattering and absorption of light. It

has been shown in works [19–24] that the presence of absorption in a matrix medium affects the efficiency of attenuation and scattering of radiation by particles in the far-field region. In absorbing matrices one should also expect a variations in the intensity and parameters of localization „of hot spots“ in the near-field region. Theoretical study of the topology of the distribution of the near field in dielectric and absorbing matrices for spherical nanoparticles of silver, gold, copper with different sizes was carried out in the works [23–25]. It was demonstrated that the maximum attainable values of the local field amplification factors depend both on the material and size of plasmonic nanoparticles and on the dielectric characterizations of the absorbing matrix.

However, the influence of matrix absorption on the spectral dependence of the integrated scattering and absorption characterizations, such as the efficiency factors of Q_{ext} attenuation, Q_{sca} , and Q_{abs} absorption and scattering in the near field region Q_{NF} have not been studied enough. A system analysis of this problem requires performing of a cycle of theoretical studies for nanoparticles with different structural and morphological characteristics in a wide range of dielectric characteristic variations of these nanoparticles and their environment. In this case (due to the undoubted practical importance of near-field effects in metal-containing nanocomposites), close attention should be paid to studying the scattering characteristics in the near-field region of a metal nanoparticle, in particular, the near-field scattering efficiency factor Q_{NF} . For spherical plasmonic nanoparticles, such calculations can be performed using formulas for the efficiency factors of attenuation and scattering by spherical particles in an absorbing matrix, proposed in the works [15–24] and based on a rigorous Mie theory.

In addition, it is now well known that in the visible region of the spectrum, the scattering and absorption characteristics of metal nanoparticles are quantitatively significantly affected by the so-called internal-size effects consisting in the dependence of complex permittivity of the nanoparticle on its size. Sufficiently correct consideration of internal-size effects for spherical nanoparticles of noble metals with sizes smaller than the free path of electrons in a massive metal sample can be performed using the Kreibig model [1,26]. This model has been successfully used to calculate the spectra Q_{ext} , Q_{sca} , Q_{abs} for spherical Ag, Au, Cu nanoparticles surrounded by a non-absorbing medium [27–29]. Similar approach was also used for hybrid nanoparticles placed in a non-absorbing medium, which represented the two-layer nanospheres with a concentric metal core and an absorbing organic shell consisting of molecular aggregates of dyes (see [30] and references therein). A modification of the Kreibig model for metal nano-shells deposited on a spherical core made of another material was proposed in [31] and used in a number of works [32,33] to calculate the scattering and absorption characteristics of metal-containing nano-shells located in non-absorbent matrices. Together with, for the case of absorbing matrices, the theoretical analysis of the contribution of the internal-size effect in metal nanoparticles has practically not been carried out and merits special

attention. At the moment, the number of publications with calculations of the scattering and absorption characteristics of metal nanospheres in absorbing matrices is very small, and, as far as we know, these don't consider the scattering efficiency factor in the near field region Q_{NF} and don't take into account the internal dimensional Kreibig effects. The exceptions are the works [23,24], in which the calculations of the characteristics Q_{ext} , Q_{sca} , Q_{abs} , Q_{NF} , taking into account internal-size effects, were performed for the specific case of placing Ag, Au, Cu nanospheres in an absorbing copper phthalocyanine matrix.

The study of the modification for the spectral and near-field characteristics of plasmonic nanoparticles placed in an absorbing matrix is necessary in the search for effective methods for controlling the stationary and dynamic spectral characteristics of plasmonic nanostructures for the purposes of nanophotonics and nanoelectronics. In the present work, such studies were carried out drawing on the example of silver nanoparticles, since it is silver nanoparticles that are characterized by the most intense resonance of surface plasmon absorption in the visible region of the spectrum. By way of example of real absorbing matrix with a dispersion of the refractive index, a matrix of nickel phthalocyanine is considered.

Calculation method

To estimate the effect of absorption of a matrix on the near-field characteristics of plasmonic nanoparticles embedded in it, let's use the scattering efficiency factor of a plasmonic nanoparticle in the near-field region Q_{NF} . The term Q_{NF} , which is representing the near-field form of Q_{sca} , was first introduced in the work [2], where the formula for calculating Q_{NF} for $R_s = R_{\text{NP}}$ for a transparent matrix, was obtained. The factor Q_{NF} characterizes the increase in the field intensity on the surface of a sphere of radius R_s when a nanoparticle is introduced into the center of this sphere. In the case of a spherical plasmonic particle located in absorbing medium, the formula for calculating the scattering efficiency factor in the near field region at a distance R_s from the center of the spherical particle has the form [23]

$$Q_{\text{NF}} = \frac{(4\pi\kappa_m R_s)^2}{\lambda_0^2 [1 + e^\beta (\beta - 1)]} \sum_{n=1}^{\infty} \left\{ |a_n|^2 [(n+1)|h_{n-1}|^2 + n|h_{n+1}|^2] + (2n+1)|b_n|^2 |h_n|^2 \right\} \quad (1)$$

where λ_0 is wavelength of the incident radiation, a_n , b_n are Mie coefficients depending on the optical constants of the particle and matrix, as well as on the diffraction parameter $\rho = 2\pi R_{\text{NP}}/\lambda_0$, R_{NP} is the particle radius, $\beta = 4\pi R_{\text{NP}}\kappa_m/\lambda_0$, κ_m is imaginary part of the complex refractive index of the matrix, h_n is spherical Hankel function of the first kind of order n . Expression (1),

first given in [23], is obtained on the basis of classical formulas for the characteristics of the scattered field in the near field region, contained, for example, in [4].

The efficiency factors for Q_{sca} scattering, Q_{abs} absorption, and Q_{ext} attenuation of plasmonic spherical nanoparticles in an absorbing matrix can be calculated using the Mie theory [15–24]. As in [23,24], we used the formulas

$$\begin{aligned}
 Q_{\text{sca}} &= \frac{4\kappa_m^2}{n_m[1 + e^\beta(\beta - 1)]} \text{Re} \left\{ \frac{1}{\kappa_m - in_m} \right. \\
 &\quad \times \left. \sum_{n=1}^{\infty} [(2n+1)(|b_n|^2 \xi_n \xi_n'^* - |a_n|^2 \xi_n' \xi_n^*)] \right\}, \\
 Q_{\text{abs}} &= \frac{4\kappa_m^2}{n_m[1 + e^\beta(\beta - 1)]} \text{Re} \left\{ \frac{1}{\kappa_m - in_m} \right. \\
 &\quad \times \sum_{n=1}^{\infty} [(2n+1)(\psi_n^* \psi_n' - \psi_n \psi_n'^* + b_n \psi_n'^* \xi_n + b_n^* \psi_n \xi_n'^* \\
 &\quad \left. + |a_n|^2 \xi_n' \xi_n^* - |b_n|^2 \xi_n \xi_n'^* - a_n \psi_n^* \xi_n' - a_n^* \psi_n' \xi_n^*)] \right\}, \\
 Q_{\text{ext}} &= \frac{4\kappa_m^2}{n_m[1 + e^\beta(\beta - 1)]} \text{Re} \left\{ \frac{1}{\kappa_m - in_m} \right. \\
 &\quad \times \sum_{n=1}^{\infty} [(2n+1)(\psi_n^* \psi_n' - \psi_n \psi_n'^* + b_n \psi_n'^* \xi_n + b_n^* \psi_n \xi_n'^* \\
 &\quad \left. - a_n \psi_n^* \xi_n' - a_n^* \psi_n' \xi_n^*)] \right\}, \quad (2)
 \end{aligned}$$

where n_m is the real part of the complex refractive index of the matrix, ψ_n , ξ_n , ψ_n' , ξ_n' are Riccati–Bessel functions and their derivatives, index * means complex conjugation.

In the case of metallic nanoparticles whose dimensions are comparable to the free path of electrons in the particle material, the optical constants included in formulas (1) and (2) are size-dependent. The effects associated with this circumstance are often called internal-size effects [1,4]. Since the optical constants of massive silver, gold, and copper in the visible region of the spectrum are fairly well described by the Drude model, the internal size effects for nanoparticles of these metals can be taken into account in the approximation of the Free Path Limitation of Conduction Electrons (FPLCE) [26].

The essence of the approximation is the assumption that the collision of free electrons with the surface of a nanoparticle becomes an additional source of their energy loss. As a result, the size-dependent damping constant is given by the expression

$$\gamma_{\text{NP}} = \gamma_0 + \frac{v_F}{L}, \quad (3)$$

where γ_0 is the damping constant for a massive sample, v_F is the Fermi velocity, L is the average path length of an electron in a particle, determined by collisions with the border. During diffuse scattering of electrons

on the surface $L = R_{\text{NP}}$. The value of additional energy losses of free electrons is the greater, the smaller the size of nanoparticles compared to the free path of electrons. The permittivity associated with the contribution of free electrons is determined by the expression

$$\varepsilon_{\text{NP}}(\omega, R_{\text{NP}}) = 1 - \frac{\omega_p^2}{\omega^2 + i\gamma_{\text{NP}}\omega},$$

where $\omega_p^2 = \frac{N_0 e^2}{m_e \varepsilon_0}$. Here ω_p is plasma frequency of massive metal, N_0 is density of free electrons, e and m_e are charge and the electron mass, respectively. The general scheme for calculating the size-dependent permittivity in the framework of ballistic theory in the FPLCE approximation is described in [29]. The results of applying this approach to silver nanoparticles are shown in Fig. 1. The optical constants of the massive silver are taken from [34]. To calculate the size-dependent permittivity of silver nanoparticles, we used the values of the parameters taken from the works [1,4,29]: plasma frequency $\omega_p = 1.38 \cdot 10^{16} \text{ s}^{-1}$, damping constant for massive metal $\gamma_0 = 2.73 \cdot 10^{13} \text{ s}^{-1}$, Fermi velocity $v_F = 1.4 \cdot 10^6 \text{ m} \cdot \text{s}^{-1}$.

As can be seen from Fig. 1, in the investigated range of nanoparticle sizes, the consideration of internal size effects most strongly affects the values of the real part of the complex refractive index n_{NP} . The imaginary part of the complex refraction index κ_{NP} depends only insignificant on the particle size.

Results of calculations and their discussion

Fig. 2 shows the spectral dependences of the factors Q_{ext} , Q_{abs} , Q_{NF} silver nanoparticles with different sizes ($R_{\text{NP}} = 10, 20$ and 30 nm), which are placed in transparent ($\kappa_m = 0$) and absorbing ($\kappa_m = 0.1$) matrices with refraction index $n_m = 1.5$. The calculations were performed out both taking into account internal size effects and without taking them into account.

As can be seen from Fig. 2, *a, d, g*, the spectra of the factors Q_{ext} , Q_{abs} , Q_{NF} nanoparticles with $R_{\text{NP}} = 10 \text{ nm}$ are characterized by the presence of a surface plasmon resonance absorption band in the $\lambda_0 \approx 405 \text{ nm}$ region, which has a dipole nature. With an increase in the size of nanoparticles, the dipole mode shifts to the long wavelength region of the spectrum. The intensity of the dipole mode depends non-monotonically on the size of the nanoparticles, reaches a maximum (for a chosen $n_m = 1.5$) for $R_{\text{NP}} \approx 10 \text{ nm}$, and decreases with a further increase in R_{NP} from 10 to 30 nm. In the spectra Q_{ext} , Q_{abs} , Q_{NF} for $R_{\text{NP}} > 10 \text{ nm}$, the appearance of quadrupole modes located in the short-wavelength region relative to the dipole mode is noted. The intensity of the quadrupole mode increases with increasing nanoparticle size. It is interesting to note that in the spectra of Q_{abs} for nanoparticles with $R_{\text{NP}} = 30 \text{ nm}$, the intensity of the quadrupole mode even exceeds the intensity of the dipole mode.

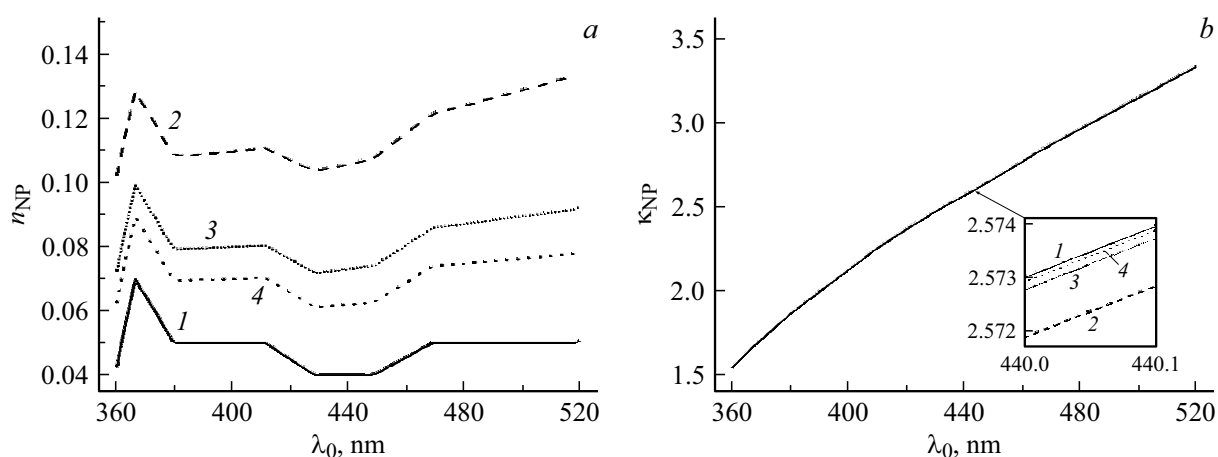


Figure 1. Spectral dependences of refraction (a) and absorption (b) indices of massive silver (1) and size-dependent refraction n_{NP} (a) and absorption κ_{NP} (b) indices of spherical silver particles with radii 10 (2), 20 (3) and 30 nm (4).

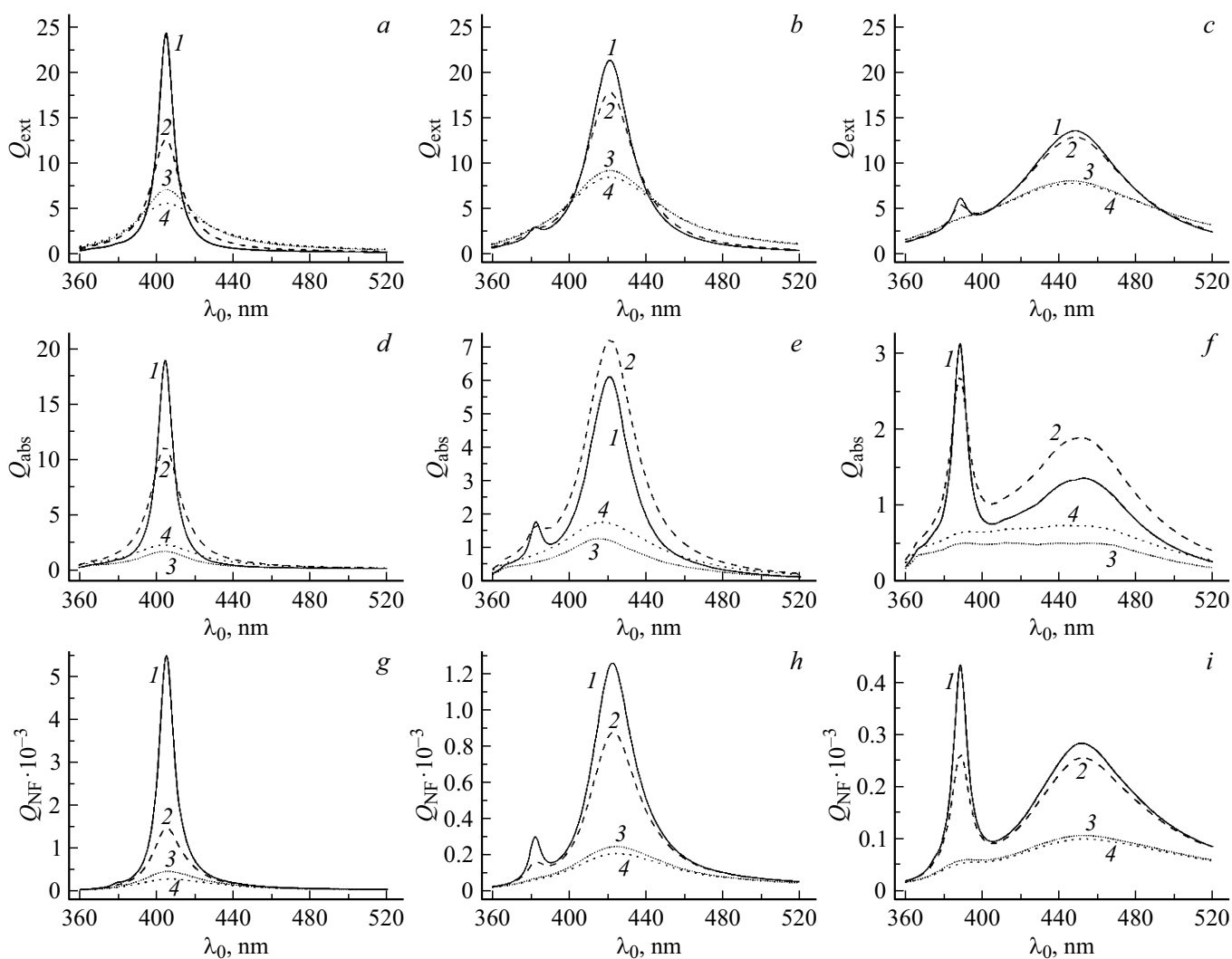


Figure 2. Spectral dependences of the attenuation efficiency factors Q_{ext} (a, b, c), absorption Q_{abs} (d, e, f) and scattering in the near field region Q_{NF} (g, h, i) for silver nanoparticles with radii $R_{NP} = 10$ (a, d, g), 20 (b, e, h), 30 nm (c, f, i) located in a matrix with refraction indices $n_m = 1.5$ and absorption indices $\kappa_m = 0$ (1, 2), 0.1 (3, 4) without taking into account (1, 3) and taking into account (2, 4) size effects.

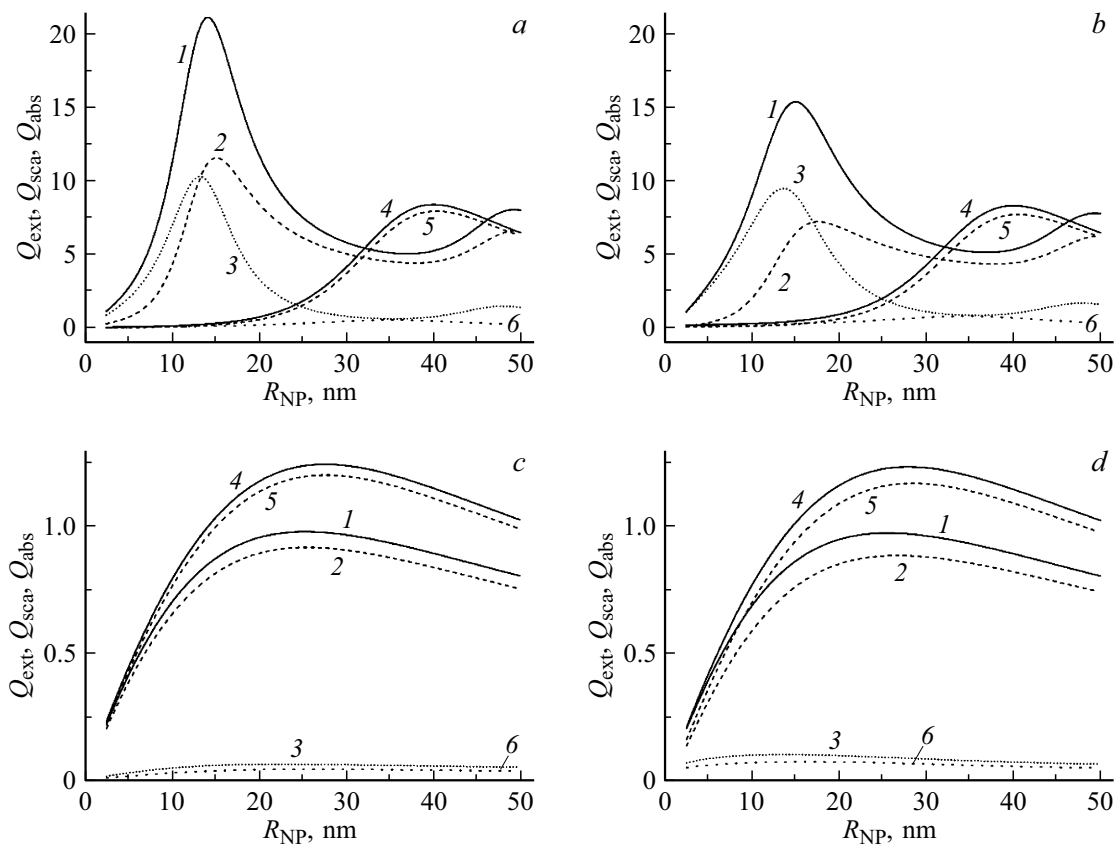


Figure 3. Dependences of the attenuation efficiency factors Q_{ext} (1, 4), scattering Q_{sca} (2, 5) and absorption Q_{abs} (3, 6) of silver nanoparticles from their radius without taking into account (a, c) and with taking into account (b, d) internal size effects. Wavelengths 410 (1, 2, 3) and 500 nm (4, 5, 6), $\kappa_m = 0.01$ (a, b) and 1 (c, d), $n_m = 1.5$.

An analysis of the data shown in Fig. 2 shows that the absorption of the matrix has almost no effect on the spectral position of the maxima Q_{ext} , Q_{abs} , Q_{NF} . However, an increase in absorption by the matrix (a change in κ_m from 0 to 0.1) leads to a strong damping of the resonances Q_{ext} , Q_{abs} , Q_{NF} due to the dipole mode and results to almost complete suppression of resonances due to the quadrupole mode.

It is important to note that taking into account the internal size effects leads to the suppression of the Q_{ext} and Q_{NF} resonances, which becomes especially noticeable with decreasing nanoparticle sizes (for $R_{\text{NP}} < 20$ nm) and decrease in absorption by the matrix. At the same time, as can be seen from Figures 2, e, f, taking into account internal size effects can lead to both a decrease and an increase in the values of the absorption efficiency factor Q_{abs} . Thus, in the spectral region of the dipole mode for particles with a radius of 20 (Fig. 2, e) and 30 nm (Fig. 2, f), a consideration of internal size effects leads to an increase in Q_{abs} both for transparent matrix and absorbing one. For a particle with a radius of 10 nm (Fig. 2, d), the effect of enhancement of plasmon absorption when internal size effects are taken into account appears only for $\kappa_m = 0.1$.

It should be clarified that the form of presentation of the results in Fig. 2 does not imply that materials with

refractive and absorption indices constant in the spectral region under consideration are having in view. The choice of the form for presenting the results of numerical calculations is caused by the multiparameter nature of the problem under consideration and seems to be the most convenient for a qualitative assessment of the influence of each of the input parameters separately. Similar representation of the results is preferable, in particular, for problems in which it is required to determine the optimal values for a certain wavelength of the optical constants of the matrix and/or the sizes of plasmonic (silver) particles. Problems of this kind arise, for example, upon laser excitation of active centers located near the surface of plasmonic nanoparticles.

Fig. 3 shows the dependences of the scattering efficiency factors Q_{sca} , absorption Q_{abs} and attenuation Q_{ext} silver nanoparticles of their sizes, calculated for wavelengths of 410 and 500 nm. The imaginary part of the refraction index of the matrices during the calculations varied in the range 0–1. The analysis was carried out for silver nanoparticles with radii of 2.5–50 nm. The calculations were performed out both taking into account internal size effects and without taking them into account. Note that matrices based on alkali-halide crystals and glasses with different concentrations of F-centers [35] can be cited as an example of materials that

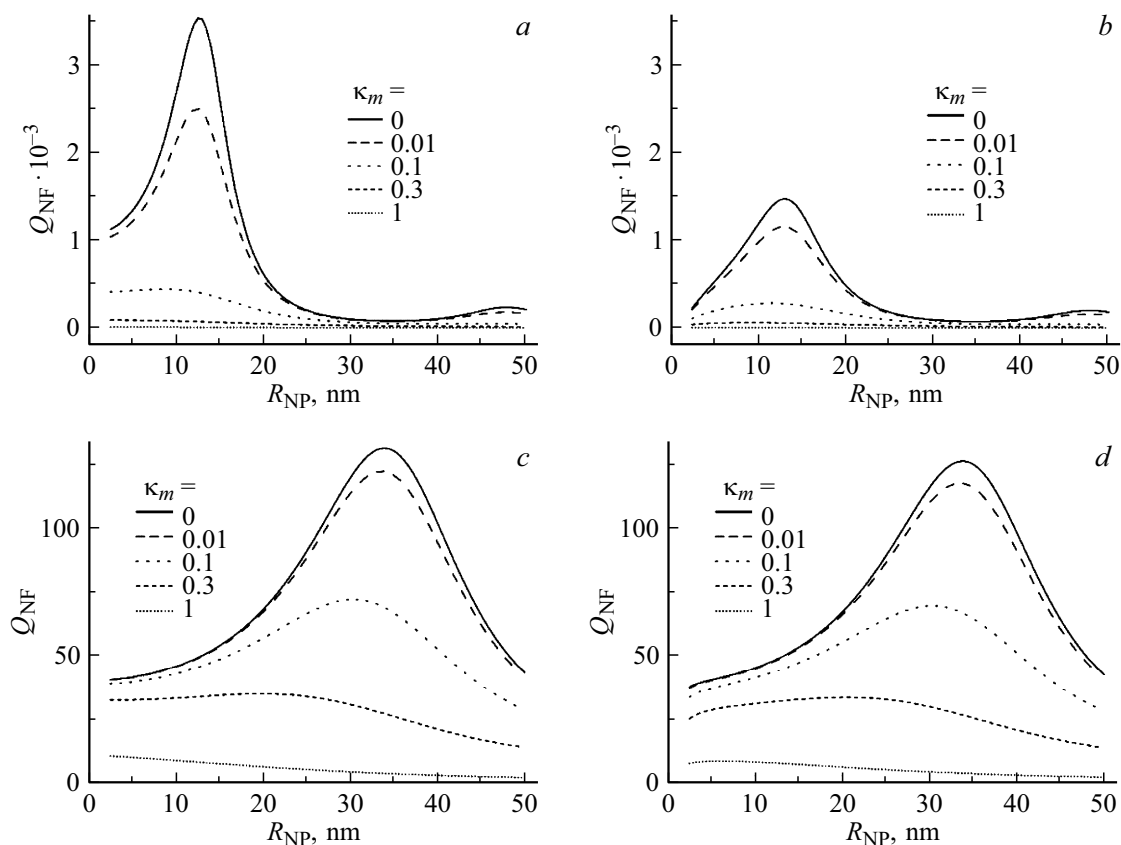


Figure 4. Dependences of the scattering efficiency factor in the near field Q_{NF} of silver nanoparticles on their radius without taking into account (a, c) and taking into account (b, d) internal size effects. Wavelengths 410 (a, b) and 500 nm (c, d), $n_m = 1.5$, $R_s = R_{\text{NP}}$.

have a fairly wide range of changes in the absorption index at a low refractive index in a certain spectral region.

As can be seen from Fig. 3, at the chosen wavelength, the dependence of the efficiency factors of absorption, scattering, and attenuation on the size of nanoparticles is non-monotonic. The position of the maxima depends both on the considered wavelength and on the absorption coefficient of the matrix. For example, at $\kappa_m = 0.01$ for a wavelength of 410 nm, the maximum values of the factors are realized near the region of sizes 12–15 nm, and for a wavelength of 500 nm they are realized near the region of sizes 35–40 nm. For $\kappa_m = 1$, both for the wavelength of 410 nm and for the wavelength of 500 nm, the maximal values of the factors are realized near the size range 20–25 nm. It should also be noted that an increase in absorption in the matrix leads to a decrease in the maximum attainable values of the factors Q_{ext} , Q_{sca} , and Q_{abs} . This effect is especially noticeable near the maximum of the SPR for a wavelength of 410 nm.

Fig. 4 shows the dependences of the scattering efficiency factor of silver nanoparticles in the near zone on their sizes, calculated for wavelengths of 410 and 500 nm. The calculation was performed for $R_s = R_{\text{NP}}$, i.e. the field enhancement was estimated directly on the surface of silver nanoparticles. As can be seen from Fig. 4, for any given particle size, an increase in the absorption of the matrix is

accompanied by a decrease in Q_{NF} . This means that, in the matrix transparency regions, the field amplification effects near the surface of the plasmonic nanoparticle are more pronounced than in the region of the absorption bands of the matrix.

It is also seen from Fig. 4 that for small $\kappa_m = 0–0.1$ the dependence $Q_{\text{NF}}(R_{\text{NP}})$ is non-monotonic. The optimal values of R_{NP} , at which the maximal value of Q_{NF} for the selected κ_m is realized, decrease with an increase in κ_m . In this case, the value of Q_{NF} also decreases at the considered wavelength. As the absorption of the matrix increases above $\kappa_m = 0.1$, the $Q_{\text{NF}}(R_{\text{NP}})$ dependence becomes monotonically decreasing.

It should be noted that for $\kappa_m = \text{const}$, the optimal value of R_{NP} essentially depends on the wavelength. Thus, at $\kappa_m = 0$ for a wavelength of 410 nm the optimal value is $R_{\text{NP}} = 10–12$ nm, and for a wavelength of 500 nm the optimal value is $R_{\text{NP}} = 33–35$ nm.

Fig. 5 shows the dependences of the scattering efficiency factor of silver nanoparticles in the near field region on the sphere radius R_s calculated for wavelengths of 410 and 500 nm and particle radii of 13 and 34 nm, respectively. The selected values of R_{NP} are optimal for the corresponding wavelengths at $\kappa_m = 0$, i.e., under the specified conditions for such R_{NP} , the value of the scattering efficiency factor in the near field region on the nanoparticle surface $Q_{\text{NF}}(R_{\text{NP}})$

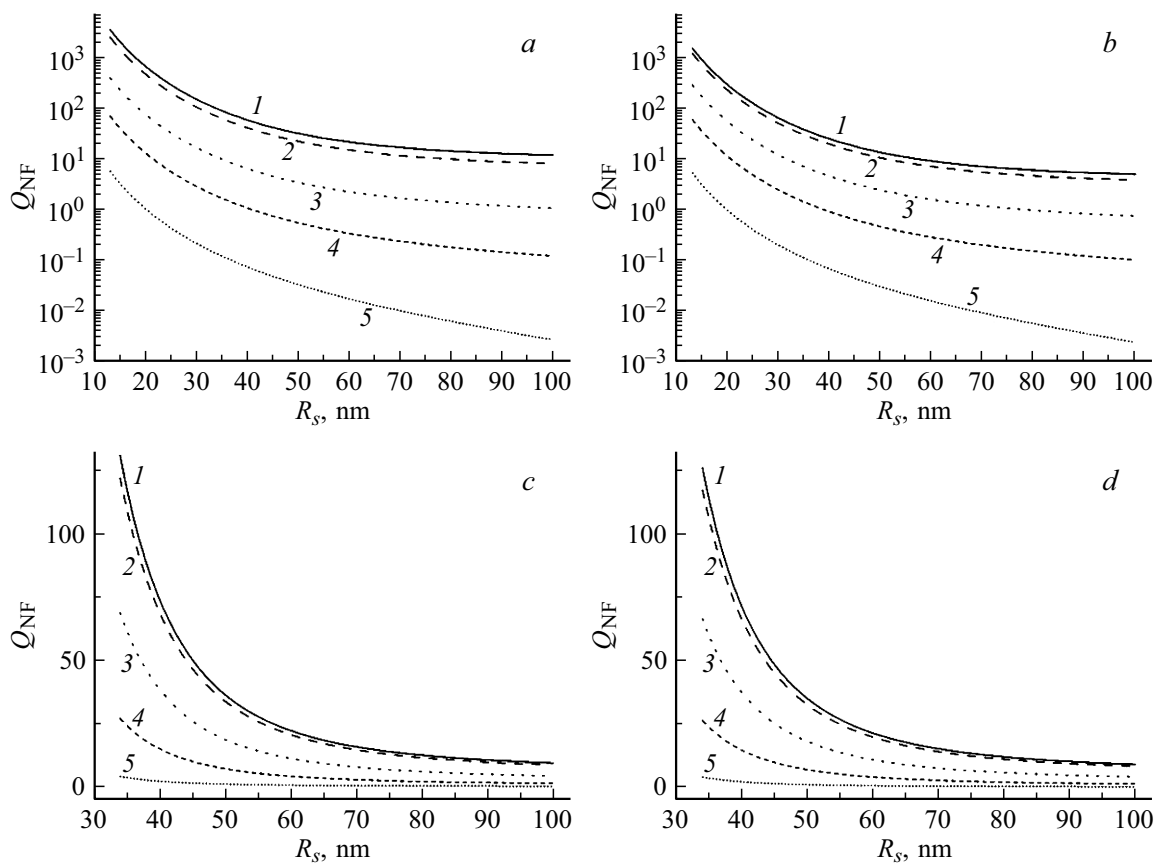


Figure 5. Dependences of the scattering efficiency factor in the near field Q_{NF} of silver nanoparticles with radii 13 (*a, b*) and 34 nm (*c, d*) on the distance R_s from the center of the nanoparticle without taking into account (*a, c*) and taking into account (*b, d*) internal size effects. Wavelengths are 410 (*a, b*) and 500 nm (*c, d*), $n_m = 1.5$.

is maximum compared to other particle sizes (Fig. 4). As can be seen from the comparison of Fig. 5, *a* and 5, *b*, taking into account internal size effects leads to a decrease in the values of Q_{NF} over the entire range R_s . The influence of internal size effects on the scattering efficiency factor in the near field region is especially strong for transparent and weakly absorbing matrices. It should also be noted that for any values of κ_m , a monotonically decreasing dependence $Q_{NF}(R_s)$ is observed in the studied spatial region.

In most applied problems of nanophotonics and nanoplasmonics, absorbing materials used as matrices for metal nanoparticles are characterized by a dispersion of the complex refractive index. For such matrices in the visible region of the spectrum, there are both absorption bands and regions of high transparency. This complicates the analysis of the features for attenuation and scattering of light by plasmonic nanoparticles in a wide range of the spectrum and requires a separate consideration for each specific material used as a matrix.

As an example, let's consider the situation when Ag nanoparticles are placed in films of nickel phthalocyanine (NiPc). This situation is of interest for photovoltaic applications, since organic semiconductors, including NiPc, are widely used in this branch. The optical constants of

nickel phthalocyanine in the visible and near-IR spectral regions are taken from [36] and are shown in Fig. 6.

As can be seen from Fig. 6, NiPc is characterized by the presence of absorption and dispersion of the refraction index both in the UV region (near the absorption band of NiPc with a maximum in the region of 340 nm), and in the visible region of the spectrum, where two absorption bands of NiPc with maxima in the region of 615 and 680 nm. It should be noted that the features of the spectral dependence of the refraction index of nickel phthalocyanine in the region of 400–500 nm, where $\kappa_{NiPc} = 0-0.1$, suggest the

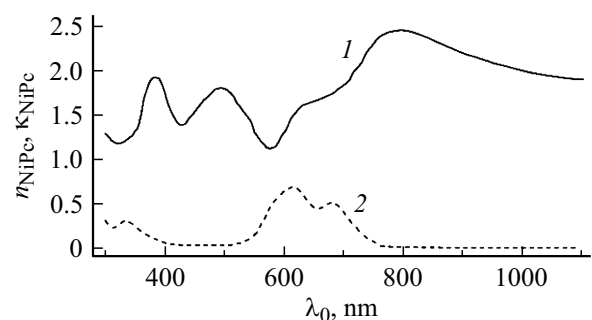


Figure 6. Spectral dependences of the refraction (*1*) and absorption (*2*) indices of nickel phthalocyanine.

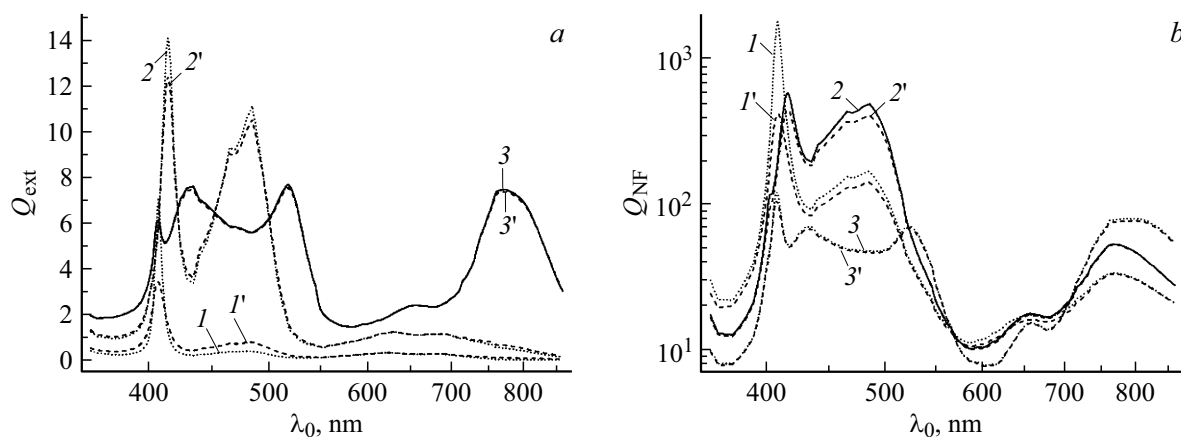


Figure 7. Spectral dependences of the attenuation efficiency factors Q_{ext} (a) and scattering in the near field region Q_{NF} (b) silver nanoparticles with radii $R_{\text{NP}} = 5$ (1, 1'), 20 (2, 2'), 40 nm (3, 3') in the nickel phthalocyanine matrix without taking into account (1, 2, 3) and taking into account (1', 2', 3') size effects.

possibility of implementing the Fröhlich condition for silver nanoparticles for two frequencies in this spectral range. This can lead to the formation of a two-peak structure of the SPR band of silver nanoparticles embedded in the NiPc matrix.

On checking purposes for this assumption, Fig. 7 shows the spectral dependences of the scattering factor in the near field region Q_{NF} and the attenuation efficiency factor Q_{ext} of silver nanoparticles in a NiPc matrix. The nanoparticle radius varied over a wide range from 5 to 40 nm.

As can be seen from Fig. 7, a, for small silver nanoparticles with a radius of 5 nm, the SPR band has a single-peak structure with a maximum in the region of 410 nm, while the one shown in Fig. 7, b spectrum of Q_{NF} for the same sizes of silver nanoparticles is characterized by a doublet structure with maxima near 405 and 480 nm. This indicates a higher sensitivity of the Q_{NF} spectra to the matrix refractive index dispersion. Note that taking into account the size dependence of the optical constants of silver nanoparticles leads to a significant decrease in the maximum achievable values Q_{ext} and Q_{NF} .

As the size of silver nanoparticles increases, the structure of the Q_{ext} and Q_{NF} spectra becomes more complicated. For $R_{\text{NP}} = 20$ nm in the spectral region 400–500 nm, a doublet structure is observed as Q_{NF} bands (maxima at 416 and 485 nm) and the Q_{ext} bands (maxima at 415 and 485 nm). These bands with a doublet structure are of a dipole nature, which is confirmed by calculations performed without taking into account the contribution of higher-order multipoles. With a further increase in the size of nanoparticles up to $R_{\text{NP}} = 40$ nm, the maxima of the doublet structure, determined by the peculiarities of the dispersion of the refraction index of nickel phthalocyanine, shift by 435 and 518 nm. Concurrently, in the long-wavelength region 700–860 nm, a band of strong attenuation by the nanoparticle of the incident radiation appears, which comes to the spectral transparency band of nickel phthalocyanine. The maximum of this band is located near 770 nm. This attenuation of radiation in the region of a high refraction

index of a nanoparticle is mainly associated with intense dipole scattering, which rapidly increases with an increase in the size of nanoparticles and monotonically weakens with a transition to a longer wavelength region of the spectrum. In addition, mode structures of the SPR band are formed, which is associated with an increase in the contribution of high-order multipoles. This leads to the appearance in the Q_{ext} and Q_{NF} spectra of a low-intensity quadrupole band with a maximum near 407 nm. When the wavelength is fixed in the spectral region near the maxima of the doublet structure, which have a dipole nature, the dependence of the efficiency factors of attenuation Q_{ext} and scattering in the near zone Q_{NF} on the size of nanoparticles, calculated taking into account internal size effects, is non-monotonic.

Conclusion

The promise of plasmonic nanocomposites for the development of new components of nanoplasmonics and nanophotonics is determined by the unique possibility of controlling their spectral-selective and spectral-kinetic characteristics by modification the nanoparticle & matrix material which forming the nanocomposite, as well as the modification the concentration, size, shape, or internal structure of metal-containing nanoparticles. When plasmonic nanoparticles are close packed, interparticle electrodynamic interactions associated with near-field scattering and coherent re-irradiation by particles of each other have the most important effect on the optical and electrophysical properties of the nanocomposite. Matrix absorption can have a significant effect on the severity of near-field interparticle interactions and on their dependence on the morphological characteristics of the composite.

In the present work, using formulas based on the rigorous Mie theory, the efficiency factors for attenuation, absorption, and scattering in the far and near field regions in the

spectral region of the surface plasmonic absorption resonance of silver nanoparticles placed in absorbing matrices, are calculated. When performing calculations, proprietary version of the program was used [37]. It is shown that an increase in the absorption of the matrix leads to a significant suppression of the Q_{ext} and Q_{NF} resonances without a significant change in their spectral position. For $\kappa_m = 0-1$ it was found that at a fixed wavelength the dependence of Q_{ext} on the size of nanoparticles is non-monotonic, and the optimal value of R_{NP} , at which the maximum possible intensity value of the maximum of the SPR band is realized for a given plasmonic material, increases with increasing absorption of the matrix. Moreover, the non-monotonic dependence of the near-field scattering efficiency factor Q_{NF} on the size of nanoparticles is observed only at low matrix absorption ($\kappa_m = 0-0.1$), and for $\kappa_m > 0.1$ in the studied range of sizes of silver nanoparticles, the dependence $Q_{\text{NF}}(R_{\text{NP}})$ is monotonically decreasing.

The dependence of the optical constants of silver nanoparticles on their sizes, caused by a decrease in the mean free electron path in nanoparticles and the associated increase in the damping constant due to the collision of electrons with the boundaries of nanoparticles, leads to an additional suppression of spectral resonances Q_{ext} and Q_{NF} . Comparison of calculations, carried out taking into account and without taking into account the size dependence of the optical constants of silver nanoparticles, shows that the relative contribution of internal size effects to the suppression of the Q_{ext} and Q_{NF} resonances decreases with increasing nanoparticle size and/or absorption matrices.

The results obtained can be used in evaluating the efficiency of using plasmonic nanostructures for the development of the hardware components of photovoltaics, in particular, active components of solar cells.

Acknowledgements and Funding

The work was funded in part by the Belarusian Republican Foundation for Fundamental Research (grant № F20EA-006).

Conflict of interest

The authors declare that they have no conflict of interest.

References

- [1] U. Kreibig, M. Volmer. *Optical properties of metal clusters* (Springer-Verlag, Berlin, 1995).
- [2] B.J. Messinger, K.U. von Raben, R.K. Chang, P.W. Barber. *Phys. Rev. B*, **24** (2), 649 (1981). DOI: 10.1103/PhysRevB.24.649
- [3] M. Quinten. *Appl. Phys. B*, **73**, 245 (2001). DOI: 10.1007/s003400100650
- [4] C. Bohren, D. Huffman. *Pogloshcheniye i rasseyaniye sveta malymi chastitsami* (Mir, M., 1986). (in Russian).
- [5] N.G. Khlebtsov, L.A. Trachuk, A.G. Melnikov. *Opt. i spektr.*, **98** (1), 82 (2005) (in Russian).
- [6] R. Cheng, T. Furtak. *Gigantskoye kombinatsionnoye rasseyaniye* (Mir, M., 1984). (in Russian)
- [7] P. Matheu, S.H. Lim, D. Derkacs, C. McPheeters, E.T. Yu. *Appl. Phys. Lett.*, **93**, 113108 (2008). DOI: 10.1063/1.2957980
- [8] K. Nakayama, K. Tanabe, H.A. Atwater. *Appl. Phys. Lett.*, **93**, 121904 (2008). DOI: 10.1063/1.2988288
- [9] C.S. Solanki, G. Beaucarne. *Energy for Sustainable Development*, **XI** (3), 17 (2007). DOI: 10.1016/S0973-0826(08)60573-6
- [10] V.N. Bogach, R.A. Dynich, A.D. Zamkovets, A.N. Ponyavina. *Physics and Chemistry of Solid State*, **12** (4), 955 (2011).
- [11] A.D. Zamkovets, A.N. Ponyavina. *Zhurn. prikl. spektr.*, **79** (6), 907(2012) (in Russian)
- [12] N.A. Toropov, E.N. Kaliteevskaya, N.B. Leonov, T.A. Vartanyan. *Opt. i spektr.*, **113** (6), 684 (2012) (in Russian).
- [13] N.A. Toropov, A.A. Starovoytov, N.B. Leonov, E.N. Kaliteevskaya, T.A. Vartanyan. *Izvestiya Vuzov. Fizika*, **55** (8/2), 234 (2012) (in Russian).
- [14] O. Stenzel, A.N. Lebedev, M. Schreiber, D.R.T. Zahn. *Thin Solid Films*, **372**, 200 (2000). DOI: 10.1016/S0040-6090(00)01029-4
- [15] M. Quinten, J. Rostalki. *Part. Part. Syst. Charact.*, **13**, 89 (1996). DOI: 10.1002/ppsc.19960130206
- [16] A.N. Lebedev, M. Gartz, U. Kreibig, O. Stenzel. *Eur. Phys. J. D*, **6** (3), 365 (1999). DOI: 10.1007/s100530050320
- [17] Q. Fu, W. Sun. *Appl. Opt.*, **40** (9), 1354 (2001). DOI: 10.1364/AO.40.001354
- [18] I.W. Sudiarta, P. Chylek. *J. Opt. Soc. Am. A*, **18** (6), 1275 (2001). DOI: 10.1364/JOSAA.18.001275
- [19] W.C. Mundy, J.A. Roux, A.M. Smith. *J. Opt. Soc. Am.*, **64** (12), 1593 (1974). DOI: 10.1364/JOSA.64.001593
- [20] P. Chylek. *J. Opt. Soc. Am.*, **67** (4), 561 (1977). DOI: 10.1364/JOSA.67.000561
- [21] R.A. Dynich. *J. Opt. Soc. Am. A*, **28** (2), 222 (2011). DOI: 10.1364/JOSAA.28.000222
- [22] M.I. Mishchenko. *Optics Express*, **15** (20), 13188 (2007). DOI: 10.1364/OE.15.013188
- [23] R.A. Dynich, A.N. Ponyavina, V.V. Filippov. *Zhurn. prikl. spektr.*, **76** (5), 746 (2009) (in Russian)
- [24] R.A. Dynich, A.N. Ponyavina, V.V. Filippov. *Opt. i spektr.*, **110** (6), 909 (2011) (in Russian).
- [25] R.A. Dynich, A.N. Ponyavina. *Zhurn. prikl. spektr.*, **75** (6), 831 (2008) (in Russian)
- [26] U. Kreibig, C.V. Fragstein. *Z. Phys.*, **224** (4), 307 (1969). DOI: 10.1007/BF01393059
- [27] A.V. Uskov, I.E. Protsenko, N.A. Mortensen, E.P. O'Reilly. *Plasmonics*, **9**, 185 (2014). DOI: 10.1007/s11468-013-9611-1
- [28] A.D. Kondorskiy, V.S. Lebedev. *J. Russ. Laser Res.*, **42**, 697 (2021). DOI: 10.1007/s10946-021-10012-3
- [29] S.M. Kachan, A.N. Ponyavina. *J. Phys.: Condens. Matter*, **14**, 103 (2002).
- [30] V.S. Lebedev, A.S. Medvedev. *Quantum Electron.*, **42** (8), 701 (2012). DOI: 10.1070/QE2012v042n08ABEH014833
- [31] S.M. Kachan, A.N. Ponyavina. *J. Mol. Struct.*, **563-564**, 267 (2001). DOI: 10.1016/S0022-2860(00)00882-6
- [32] T.V. Teperik, V.V. Popov, F.J. Garcia de Abajo. *Physical Review B*, **69**, 155402 (2004). DOI: 10.1103/PhysRevB.69.155402
- [33] B.N. Khlebtsov, V.A. Bogatyrev, L.A. Dykman, N.G. Khlebtsov. *Opt. i spektr.*, **102** (2), 269 (2007) (in Russian).

- [34] P.B. Johnson, R.W. Christy. *Phys. Rev. B*, **6** (12), 4370 (1972). DOI: 10.1103/PhysRevB.6.4370
- [35] A.S. Marfunin. *Spektroskopiya, lyuminestsentsiya i radiatsionnyye tsenry v mineralakh* (Nedra, M., 1975) (in Russian).
- [36] M.M. El-Nahass, K.F. Abd-El-Rahman, A.A.M. Farag, A.A.A. Darwish. *Intern. J. Modern Physics B*, **18** (3), 421 (2004). DOI: 10.1142/S0217979204023982
- [37] R.A. Dynich. *Certificate of voluntary registration and depositing of the copyright object/related rights object*. NATIONAL CENTER OF INTELLECTUAL PROPERTY OF THE REPUBLIC OF BELARUS, 1519-CP (2022).